NASA TM X- $\times 0449$

A DIRECTIONAL LOW ENERGY GAMMA-RAY DETECTOR

G. MORFILL
G. F. PIEPER

SEPTEMBER 1973

GSFC —— **GODDARD SPACE FLIGHT CENTER**
GREENBELT, MARYLAND

A DIRECTIONAL LOW ENERGY GAMMA-RAY DETECTOR

G. Morfill and G. F. Pieper[*]

Max Planck Institüt für Extraterrestrische Physik
8046 Garching bei München, W. Germany

*Permanent address: Goddard Space Flight Center
                     Greenbelt, Maryland U.S.A. 20771

/

Abstract

The sensitivity of a directional gamma-ray detector, which relies on blocking a source to determine its direction and energy spectrum, is calculated and compared to the more conventional well-shaped shielded detectors. It is shown that such an 'anticollimator' detection system provides a basis for measuring the celestial diffuse gamma-ray background, gamma-ray sources and bursts with good energy, angular, and time resolution, and that additionally the system is 20 to 50 times as sensitive as conventional detectors when compared on a per unit mass basis.

Introduction

Important outstanding problems in gamma-ray astronomy today are the accurate determination of the diffuse gamma-ray background and its degree of isotropy[1], the location and energy spectra of possible gamma-ray sources[1], and measurement of the energy spectra of bursts[2] which are possibly due to emissions from flare stars[3].

The experimental requirements for the three areas of research mentioned above are different; the background measurement requires a good knowledge of the detector efficiency and spacecraft absorption and background, as well as the long-time accumulation of data, the anisotropy and source measurements require the detector to have good directionality which is then employed in an all-sky survey, and the measurements of bursts require in addition to directionality good temporal resolution.

It can be shown that a single experimental setup, which relies on an anticollimation technique, provides optimum or near optimum possibilities for new measurements in the above problem areas.

Description of the Detector Concept

This paper describes a directional low energy gamma-ray detector (> 200 keV to < 30 MeV) of high sensitivity. Gamma rays in the energy range discussed have very small absorption coefficients, even in detectors of high atomic mass (e.g. CsI or NaI), so that large amounts of scintillator are needed to absorb them.

The merits of the detector outlined below are summarized as follows:

1) The detector is highly directional ($\sim 6^{\circ}$) and can resolve closely-spaced sources.

2) The detector is able to measure the diffuse omnidirectional background since it does not have a collimator and, therefore, a complicated transmission function. Thus it is possible to measure sources and background both efficiently with the same instrument.

3) Compared to conventional detectors (active collimator systems) an increase in sensitivity of a factor 20 - 50 is achieved for the same detector mass in the important energy range 1 MeV - 15 MeV.

4) The detector consists of six independent units, and has, therefore, a large degree of redundancy without affecting detector performance significantly (15% reduction in sensitivity if one unit fails).

5) Modulation of the source is achieved five times for each unit during a satellite spin period, so that time variation (due to e.g. solar X-ray events) in the background flux can be eliminated.

6) Fast time resolution is required for scanning directionality, with data accumulated in various spin sectors (e.g. 120 sectors 3° wide). It is easy to compare the total measured counting rate during such a spin sector with a (variable) threshold level, for separate storage in the case of an anomalous increase in intensity.

The detector suffers from induced radioactivity background[4] just like any other alkali halide detector system which does not rely on coincidence measurement. In order to obtain maximum sensitivity and minimum background due to this source, an orbit similar to that of ERS 18 (perigee 3 R_E, apogee 18 R_E) is required, or alternatively an equatorial low altitude (< 450 km) orbit, which always remains below the radiation belt may be used. Atmospheric gamma rays might be a further source of background in the low altitude orbit, and would make measurement of the diffuse flux more difficult.

Measurements of radiations from distant astronomical sources usually involve orienting a detection device to intercept a parallel beam of the radiation. Frequently the detection device is sensitive to background radiations from other than the desired direction, necessitating that a shielding material be placed around the detector to absorb radiations from all directions except the desired one. In the case of visible

light or other easily absorbed radiations, a passive shield
can be used with little weight penalty. For X- and gamma-
rays of a penetrating nature, an active shield must be used in
anticoincidence with the detector to eliminate radiations
partially absorbed in the shield (e.g. Compton scattered)
or secondary effects (e.g. K-X-rays). Such a shield can impose
a severe weight penalty on the detector system and can still
serve as a source of additional background from the decays
of radioactivities created in the shield.

An alternate system, which may be called an "active
anticollimator" has been suggested[5,6]. Its properties turn
out to be considerably more satisfactory for low energy gamma
rays (0.1 - 10 MeV) than those of an active collimator. The
active anticollimator (AAC) consists of an array of n identical
alkali halide detectors arranged in a regular manner evenly
spaced along the circumference of a circle. (See Fig. 1.)
Each detector crystal is a cylinder R cm in radius and 2R
high. The axes of the cylinders are all parallel to each
other, perpendicular to the plane of the circle. The whole
system rotates about an axis through the center of the circle,
also perpendicular to the plane of the circle. Imagine the
spin axis of the system oriented so that radiation from the
source being investigated enters in the plane of the circle.

Then each detector will be blocked successively by the other detector crystals and a modulation of its counting rate will occur. We wish to determine the amplitude of this modulation and to compare the AAC system to the AC system on a per unit mass of detector basis.

1) AAC System

We consider first, for simplicity, a two-detector system, consisting of two spherical detectors of radius R separated by a distance M. For additional simplicity in presentation, we assume here that all radiations pass through the center of each spherical crystal. (The situation is changed quantitatively ($\sim$ 30%), but not qualitatively when off-center radiations are included.) We shall measure the number of counts, N_S, from a distant source of energy spectrum $F_S(E) \frac{photons}{cm^2 \, sec \, MeV}$ in a time Δt when the source can be seen clearly by one detector and the number of counts, N_S', in an equal interval Δt when the source is occulted by ther other detector. In both cases, an isotropic background of spectrum $F_B(E) \frac{photons}{cm^2 \, sec \, ster \, MeV}$ will produce N_B counts in Δt. For the modulation to be significant to 3 standard deviations, the difference between the occulted and non-occulted numbers of counts must satisfy the ratio

$$R_a = \frac{N_S + N_B - N_S' - N_B}{[N_S + N_B + N_S' + N_B]^{1/2}} \geq 3 \qquad (1)$$

In the energy interval ΔE, we have

$$N_S(E) \; \Delta E = F_S(E) \; \pi R^2 \; \Delta t \; (1 - e^{-2\mu(E)R}) \; \Delta E \qquad (2)$$

$$N_S'(E) \; \Delta E = F_S(E) \; \pi R^2 \; \Delta t \; (1 - e^{-2\mu(E)R}) e^{-2\mu(E)R} \; \Delta E \qquad (3)$$

and

$$N_B(E) \; \Delta E = F_B(E) \; \pi R^2 \; \Delta t \; (4\pi - d\Omega + d\Omega \, e^{-2\mu(E)R})$$
$$(1 - e^{-2\mu(E)R}) \; \Delta E \qquad (4)$$

where $\mu(E)$ is the linear absorption coefficient for gamma radiation in the detector and $d\Omega = \pi R^2/h^2$ is the solid angle subtended by one detector at the other. It is a good assumption in all cases that $d\Omega \ll 4\pi$. We also assume N_S and N_S' are $\ll N_B$ (or $4\pi F_B \gg F_S$). With these assumptions, the ratio becomes

$$R_a = \frac{F_S\sqrt{\Delta t}}{2\sqrt{2F_B}} \; R \; (1 - e^{-2\mu R})^{3/2} \qquad (5)$$

It is easy to extend this calculation to the case of n detectors in a regular array, as in Fig. 1. Since the source can either be seen by a given detector or be occulted by only one other detector at one time, neither N_s nor N_s' is changed. The background count N_B is changed by replacing $d\Omega$ by $n \cdot \overline{d\Omega}$, but the final result for R_a remains unchanged if $n \cdot \overline{d\Omega} \ll 4\pi$ remains a valid assumption.

The effect of additional detectors is felt in the time. Out of a total viewing time T (= many system spin periods), source occultations with n detectors occur for a time $\Delta t = \frac{\overline{\alpha}}{360} \cdot T \cdot n \cdot (n - 1)$, where $\overline{\alpha}$ is the mean full width at half maximum angle subtended by one detector at another. We may now write for R_a

$$R_a = \frac{F_s \sqrt{\frac{\overline{\alpha}}{360} T}}{2\sqrt{2} \; F_B} \; \sqrt{n(n-1)} \; R \left(1 - e^{-2\mu R}\right)^{3/2} \tag{6}$$

from this we define G, the geometric factor for an array of n detectors of radius R

$$G = \sqrt{n(n-1)} \; R \; (1 - e^{-2\mu R})^{3/2} \tag{7}$$

Figures 2 and 3 show the properties of this factor as a function of μ, R, and n. In all cases, the variable n or R is suppressed in favor of the total volume of the detector system in order to facilitate later comparison with the AC system. Fig. 2 shows the effect of increasing the number of detector spheres at an intermediate value of μ, and Fig. 3 shows the dependence of G on volume for a system of 6 spheres at various values of μ. The effect of the nearly total absorption of incoming radiation at large radius and high μ is clear. It turns out that a system of 6 detectors appears most reasonable if detectors identical to the Apollo 15 and 16 detectors are used (R $\cong$ 4.5 cm) and the enveloped arrangement is confined to a Scout shroud size.

2. AC System

The active collimator (AC) system is shown in Fig. 4. The analysis is similar to that for the AAC. When the source is visible in the detector opening,

$$N_S(E)\ \Delta E = F_S\ (E)\ \pi\ (R-x)^2\ \Delta t\ (1-e^{-2\mu(R-x)})\ \Delta E \tag{8}$$

when the source is invisible,

$$N_S'(E)\ \Delta E = N_S(E)\ e^{-\mu x}\ \Delta E \tag{9}$$

In both cases, the background counts will be

$$N_B(E) \; \Delta E = F_B(E) \; \pi \; (R-x)^2 \; \Delta t \; (1-e^{-2\mu(R-x)})$$

$$(dr + (4\pi - d\Omega) \; e^{-\mu x}) \; \Delta E \qquad\qquad (10)$$

Here again $\mu = \mu(E)$, and $d\Omega = \pi \; (R - x)^2/1^2$ is the solid angle of opening of the AC. Using the same assumptions as previously, $d\Omega \ll 4\pi$ and $4\pi \; F_B \gg F_s$,

$$R_a = \frac{F_s \sqrt{\Delta t}}{2\sqrt{2} \; F_B} \; (R-x) \; (1-e^{-2\mu(R-x)})^{1/2} \; (1-e^{-\mu x}) \; e^{\mu x/2} \qquad\qquad (11)$$

The geometric factor for this system is then

$$G = (R-x) \; (1 - e^{-2\mu(R-x)})^{1/2} \; (1 - e^{-\mu x}) \; e^{\mu x/2} \qquad\qquad (12)$$

It is necessary first to optimize the value of x. Fig. 5 shows this optimization, plotting G vs. x for constant μ. When μ is small, the maximum in G is very flat, so it would be quite acceptable in practice to choose a constant value of x for all μ appropriate to a higher value of μ. In the calculations actually done, the optimum value of x was used for each value

of μ. The properties of the AC system as a function of detector volume for various values of μ are shown in Fig. 6. This figure shows that the AC system has large values of G only for large μ and large volumes.

Comparison of AC and AAC Systems

1. Sensitivity

The AC and AAC systems are compared in Fig. 7, for an AAC system of 6 spheres of radii 3, 4, or 5 cm, each with an AC system of approximately equal volume, i.e., the AAC system of 6 spheres of R = 4 cm has a volume of 1608 cm^3 and should therefore be compared with the AC system of R = 5 cm, whose volume is 1586 cm^3, etc. In each case, the clear superiority of the AAC system at lower values of μ is evident. It is also clear that at higher values of μ than shown in Fig. 7, the AC system will have the advantage, e.g. at $\sim$ 40 kev the AC system will be superior, corresponding to the active shield's being a real total absorber and removing the background. Thus the AC and AAC systems are complementary, with the cross over point between them being approximately 200 kev, where the photoelectric absorption becomes small.

We wish now to compare the AC and AAC systems against the radiation from a known source, the Crab Nebula, whose energy spectrum is given quite accurately by

$F_s(E) = 0.9 \times 10^{-2} E^{-2} \dfrac{\text{photons}}{\text{cm}^2 \text{ sec MeV}}$. For a 3 standard

deviation observation, we have

$$F_s^* = \frac{6\sqrt{2\ F_B}}{G\sqrt{\dfrac{\bar{\alpha}}{360}}\ T} \qquad\qquad (13)$$

where F_s^* is the minimum resolvable photon flux from a

source. We take[1] $F_B = 0.026\ E^{-2}$ photons/cm^2 sec ster MeV,

thus

$$F_s^* = \frac{26}{G \cdot E\sqrt{\bar{\alpha}T}} \qquad\qquad (14)$$

with $\bar{\alpha}$ in degrees, T in seconds, E in MeV and G in cm.
Choosing $\bar{\alpha} = 7^o$ and T = 1 day = 8.64 $\times 10^4$ sec, we have

$$F_s^* = \frac{3.34 \cdot 10^{-2}}{E \cdot G(E)} \qquad\qquad (15)$$

The results for an AAC system of R = 4 cm, n = 6 spheres,
($\therefore$ volume = 1608 cm^3) for both NaI and CsI are shown in
Fig. 8 along with the result for an AC system of comparable
volume ($\approx$ 1586 cm^3). The results show that the Crab should

be observable to about 3.7 MeV (a flux of $\sim 7 \times 10^{-4}$

protons/cm^2 sec MeV) using an AAC system of R = 4 cm,

n = 6, and thus volume 1608 cm^3, a mass therefore of 7.25

kg CsI. The AC system can see the Crab above background

only to 600 kev (a flux of $\sim 2.5 \times 10^{-2}$ photons/cm^2 sec MeV)

with an approximately equal volume, 1586 cm^3, and a mass of

7.15 kg CsI.

@. Angular and Energy Resolution

The spacing of some of the strongest X-ray sources near

the galactic center is close enough to require an angular

resolution of $\sim 5^{\circ}$ to 7° at full width half maximum, in order

to resolve them. Both detector systems (AC and AAC) were

therefore chosen to have angular resolutions of 7° FWHM.

(Counts in the AAC detector should be accumulated in spin

sectors of angular width $\lesssim$ 1/2 times the detector angular

resolution, i.e. in this case $\sim 3^{\circ}$. This is necessary in

order not to smear out the modulation in detector counting

rates introduced by source occultation. If the satellite spin

rate is w revolutions/minute, the time spent in accumulating

data in the same spin sector of 3° width is $\frac{1}{2w}$ seconds

during one satellite revolution.)

Modulations in count rate due to an uneven mass

distribution in the spacecraft can be detected in the AAC

system (a single detector system would not be able to do this)

and can be removed, as they would not, in general, have the

same characteristics as a source modulation.

Energy resolution depends on the crystal size; a large crystal will minimize electron escape and lead to a larger photopeak, especially for incident gamma rays of high energy. The AAC system employs larger detecting crystals than the optimum design AC system of the same mass. Thus the energy resolution of the AAC system should be better at large energies than that of the AC system, although the active shield will reduce the size of the Compton plateau in the latter system and thus emphasize the importance of the photopeak again. At ~ 10 MeV energies, the AC system will become very inefficient due to high energy electron escape.

3. Burst Detection

The observed gamma-ray bursts[2] last for times up to ~ 30 seconds during which the X-ray counting rates have exceeded the background rates by factors of 10 or more. Clearly it is important to measure accurately the direction of arrival of these photons as well as their energy spectra in order to learn something about their origin. This requires a fast reaction time to measure a statistically significant increase in the counting rate. The fastest time division required for angular resolution is the accumulation time during one spin sector, i.e. $\frac{1}{2w}$. This interval may be subdivided further for the purposes of fast burst detection. Comparison of the total integrated count rates of all crystals in the AAC with a programmable reference rate should ensure that bursts can be

detected within a small fraction of a second and that the period
of enhanced counting rate during the burst is stored separately
for energy spectral analysis. If the 'burst' radiation lies
in AAC system plane, its direction can be determined to an
accuracy of a few degrees, if the burst lasts longer than $\frac{1}{w}$
seconds, where w is the spacecraft spin rate in revolutions/
sec. If the sources of these bursts are randomly spaced,
the probability of one of them being observed while it is
coplanar with the AAC system (within the detector resolution)
is given by

$$P = \frac{\bar{\alpha} \cdot 2\pi}{4\pi} = \frac{\bar{\alpha}}{2} \tag{16}$$

For $\bar{\alpha} = 7^{O}$, $P \approx 3\%$. It is likely that many of these gamma
ray burst sources lie in the galactic plane, thus P should
be substantially greater than 3% during a galactic plane
scan, which would initially fix such source locations to
within a few degrees with a single AAC detection system.
Greater angular resolution can be obtained by triangulation
of path lengths using several well separated spacecraft.

Conclusions

We have shown that a gamma-ray detector system can be constructed, which works on an anticollimation principle (AAC) and which has good properties for the measurement of the diffuse celestial background gamma-ray energy spectrum, the measurement of the energy spectra of discrete sources including the recently observed gamma-ray bursts. The system has good sensitivity, angular, energy and time resolution.

References

(1) Proceedings of the International Symposium and Workshop on Gamma-Ray Astrophysics, Goddard Space Flight Center, preprint X-641-73-180, June 1973.

(2) Klebesadel, R. W., I. B. Strong and R. A. Olsen, Astrophys. J. Lett. 182, L85, 1973.

(3) Stecker, F. and K. Frost, Nature, to be published, 1973.

(4) Dyer, C. S. and G. E. Morfill, Astrophysics and Space Science 14, 243, 1971.

(5) Morfill, G. E., Ph.D. Thesis, Imperial College of Science and Technology, London, 1971.

(6) Morfill, G. E. and G. F. Pieper, Jahresbericht 1972, Max-Planck Institut fur Extraterrestrische Physik, Garching b. Munchen, W. Germany.

Figure Captions

Figure 1   Schematic diagram of the active anti-collimator

detector assembly, viewed from an angle above the

rotation plane. A is the absorber and D the

detector crystal for the source position shown.

Figure 2   Active anti-collimator 'geometric factor' G (see

text), which is a measure of detector sensitivity,

as a function of total detector volume (proportional

to detector mass). 'n' is the number of crystals

used, and μ (cm^{-1}) is the absorption coefficient.

This figure shows that asymptotically, G increases

linearly with detector volume, independent of n,

the number of detectors. It is then more efficient

to increase n rather than the size of the

individual crystals.

Figure 3   'Geometric factor' G (see text) for the active

anti-collimator case of six crystals, discussed

in the text, as a function of total detector volume
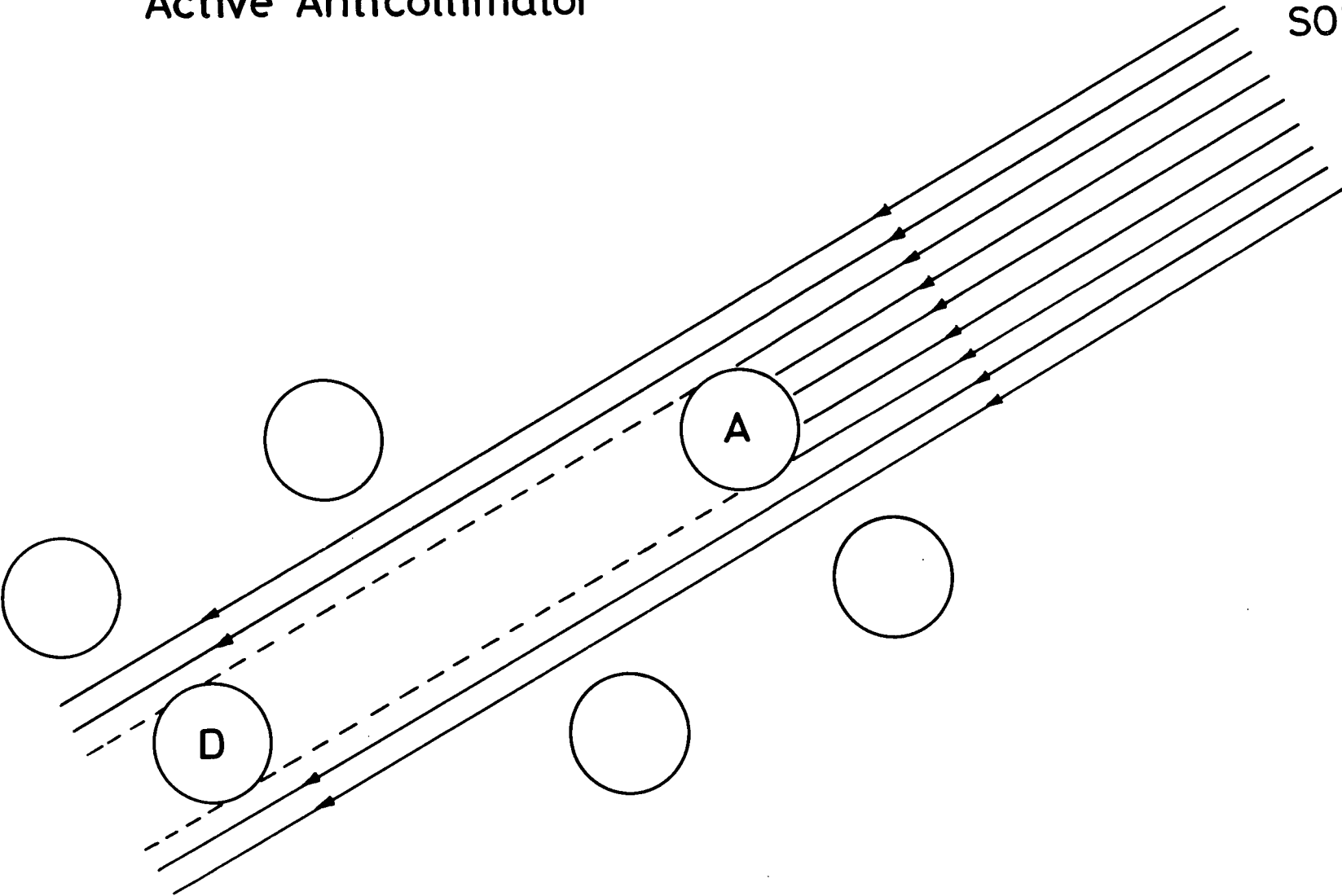
and absorption coefficient μ (cm^{-1}).

Figure 4   Diagram of the active collimator (AC) assembly chosen for comparison with the active anticollimator (ACC) system. l is the length of the collimator, h_{pm} the height of the inside photomultiplier (taken to be 5 cm).

Figure 5   'Geometric factor' G (see text) for the active collimator at various absorption coefficients μ. This figure shows that, at given μ, an optimum collimator thickness can be calculated which yields the greatest sensitivity (largest G). The total detector mass has been held constant (R = 5 cm).

Figure 6   'Geometric factor' G (see text) for the optimum design (see Figure 5) active collimator (AC) system as a function of total detector volume. G is plotted for various absorption coefficients u (cm^{-1}) as in Figure 3 for the case of the active anticollimator. Note the very slow increase in sensitivity for low u values even for volumes corresponding to very large detector masses.

Figure 7   Comparison of active collimator (AC) and

active anticollimator (AAC) sensitivities as

a function of absorption coefficient μ. This

figure shows that the AAC system increases

in sensitivity more rapidly at low μ (< 0.4

cm^{-1}) than the AC system, whereas at larger

μ (> 0.5 cm^{-1}) this situation is reversed.

Thus the AAC system is more sensitive in the

gamma ray region.

Figure 8   Comparison of the sensitivities of an

optimum design active collimator (AC) with an

active anticollimator system (AAC) consisting

of 6 right circular cylinders of length and

diameter 8 cm. The minimum detectable source

strength to 3 standard deviations is shown,

as well as the extrapolated Crab X-ray spectrum

for comparison.

Active Anticollimator

SOURCE

A

D

Active Anticollimator

G

VOLUME, cm³

22

Active Anticollimator

n = 6

G

$\mu = .8\ cm^{-1}$

$\mu = .3\ cm^{-1}$

$\mu = .2\ cm^{-1}$

$\mu = .1\ cm^{-1}$

VOLUME, cm^3

23

l

$\dfrac{x}{2}$

R

$R-x$

h_{PM}

x

PM

PM

Active collimator
R = 5 cm
(photom. height 5 cm
 FWHM 7 deg.)

$\mu = .7 \ cm^{-1}$

$\mu = .6 \ cm^{-1}$

$\mu = .5 \ cm^{-1}$

$\mu = .4 \ cm^{-1}$

$\mu = .3 \ cm^{-1}$

$\mu = .2 \ cm^{-1}$

$\mu = .1 \ cm^{-1}$

$x \ [cm]$

ACTIVE COLLIMATOR

$\mu = .8\,cm^{-1}$

$\mu = .6\,cm^{-1}$

$\mu = .3\,cm^{-1}$

$\mu = .1\,cm^{-1}$

VOLUME, cm^3

Active anticollimator
6 spheres

R = 5cm
vol = 2618 cm³

R = 4 cm
vol = 1608 cm³

R = 3 cm
vol = 679 cm³

R = 6 cm
vol = 2630 cm³

R = 5 cm
vol = 1586 cm³

R = 4 cm
vol = 850 cm³

Active collimator

absorption coefficient, μ cm⁻¹

SOURCE SPECTRUM

$9 \times 10^{-3} E^{-2} \dfrac{\text{photons}}{\text{cm}^2 \text{sec MeV}}$

Min. detectable source
active collimation
system
vol ≈ 1586 cm^3
R = 5 cm

Min. detectable source
anticollimation system
vol ≈ 1608 cm^3
R = 4 cm
n = 6

Fs

Na I

Cs I

Na I

Cs I

PHOTONS/cm^{2}secMeV

PHOTON ENERGY
MEV

NASA-GSFC